Chapter 12

Plasmonic Effect in Photoelectrochemical Cells

Abdul Kariem Bin Mohd Arof and
Mohd Hamdi Bin Ali Buraidah

Additional information is available at the end of the chapter

http://dx.doi.org/10.5772/intechopen.79580

Abstract

Two types of third-generation photovoltaic (PV) cells are sensitized by dyes and quantum dots (QDs), the former being dye-sensitized solar cell abbreviated as DSSC. The second is the quantum dot-sensitized solar cell or QDSSC. There are three main components in DSSC and QDSSC. The photoanode is the component where the light is being absorbed either by molecules of the dye or by the quantum dots (QDs). The sensitizers are attached on the semiconductor (normally TiO_2) surface. The conduction band (CB) of the semiconducting material should be at a level lower than the lowest unoccupied molecular orbital (LUMO) of the dye molecules or CB of QDs for fast electron transfer. Incorporation of plasmonic materials into the photoanode can increase light absorption efficiency by surface plasmon effect and thus improve the efficiency of the DSSCs and QDSSCs. Plasmonic materials that have been employed include gold (Au), silver (Ag) and aluminum (Al) nanoparticles (NPs). Different NPs exhibit different effects on the cell parameters. Covering the NPs with a thin wide bandgap semiconducting film is necessary to protect the plasmonic NP materials from the corrosive nature of the electrolyte.

Keywords: DSSC, QDSSC, plasmon surface

1. Introduction

One of the cleanest technologies that convert sunlight into electricity is the DSSC. The research on PVs has been conducted for over a century. The first commercial silicon solar cell was produced over six decades ago. Until now, 90% of the global photovoltaic market has been dominated by silicon-based solar cells. There are several solar cell technologies. Silicon wafer-based solar cell falls under the class of first-generation photovoltaic cells, which are expensive although the price has decreased. The second-generation solar cell comes with the purpose to further reduce the production cost. The third-generation photovoltaic (PV) cells are expected to

be even cheaper. The third generation is based on thin films similar to second-generation solar cells. QDSSC, DSSC, perovskite, and organic PVs are third-generation solar cells. The drawback of thin-film cells is that if the thin layer photoactive semiconductor is impinged by photons of energy similar to that of the semiconductor energy gap, the photons are only partially absorbed. One of the promising methods to improve photon absorption is by employing plasmonic materials. Plasmonic materials are metals having negative dielectric constant. Plasmonic materials in solar cells can amplify electromagnetic field, trap, and scatter light strongly to the sensitizer. In this chapter, the effect of plasmonic materials on solar cell performance will be discussed.

2. Enhancement mechanism of plasmonic materials

A plasmon is a quasi-particle that can be described by oscillations of a collection of free charges (electrons). Plasmons at the boundary of a metal and a dielectric are called surface plasmons. When the oscillation frequency of conducting electrons equals that of the incoming light, surface plasmon resonance (SPR) occurs, and a strong electromagnetic field with energy greater than that of the incident photons is generated near the nanoparticles (NPs) and is referred to as the 'near electric field'. The non-propagating excited surface plasmon in plasmonic materials is referred to as the localized surface plasmon resonance (LSPR). Size and geometry of the plasmonic NPs influence LSPR. For example, the LSPR is red-shifted if the NP size is increased. This will lead to the increase in electric field wavelength. The dielectric materials surrounding plasmonic NPs also affect the frequency of LSPR (ω_{LSPR}) [1] as can be described by Eq. (1):

$$\omega_{LSPR} = \omega_p \left(\frac{1}{1 + 2\varepsilon_m} - \frac{1}{\omega_p^2 \tau^2} \right)^{1/2} \tag{1}$$

The free electrons in the metallic NPs have a plasma frequency of ω_p. τ is electron relaxation time and ε_m is dielectric constant of the semiconducting materials. The LSPR frequency is red shifted when ε_m increases. Surface plasmon polaritons (SPPs) are created when the electromagnetic field of incident light is combined or coupled with the plasmon. The SPPs propagate along the metal/dielectric interface. In addition, incident photons are efficiently scattered by plasmonic or metal NPs depending on their geometry and size. In general, there are three ways in which plasmonic materials can affect the performance of DSSCs and QDSSCs:

i. By LSPR where the metal NPs act as subwavelength antennas through an oscillation of strong conducting electrons

ii. By SPP where the incoming light is trapped and promotes more light to be absorbed in the photoactive semiconductor

iii. By increasing light scattering and number of optical pathways

3. Structure and mechanism of DSSC and QDSSC

The main components of a DSSC are as shown in **Figure 1**. The photoanode which absorbs incident light and separates the charge is made up of a substrate (either glass or plastic). The substrate is coated on one side by a conducting oxide that is transparent. Hence, the substrate is referred to as transparent conducting oxide (TCO) substrate. The conducting oxide can be either fluorine doped tin oxide (FTO) or indium tin oxide (ITO). The TCO is coated with a semiconducting oxide layer (typically titanium dioxide (TiO_2)) and a sensitizing dye. The counter electrode (CE) is where charges (electrons released by the sensitizer) are collected from the photoanode. CE comprises TCO coated with catalyst materials. The catalyst material can be platinum (Pt), carbon, conducting polymer, metal oxide or metal carbide. The electrolyte contains a redox couple. The iodide/triiodide $\left(I^-/I_3^-\right)$ couple is an example. For solid or gel electrolytes, the ion-conducting medium is placed between the photoanode and CE. Details of the DSSC working principle are as follows:

When the DSSC is illuminated, the sensitizing dye molecules D, on the TiO_2 surface are excited D^* upon absorbing photons (Eq. 2) The excited molecules are immediately oxidized, D^+. The released electrons are driven into the CB of TiO_2 (Eq. 3). This can occur only if LUMO of the dye is at a higher position than the TiO_2 Fermi level.

$$D + h\upsilon \rightarrow D^* \tag{2}$$

$$D^* \rightarrow e^-{}_{(TiO_2)} + D^+ \tag{3}$$

The electrons that have entered the CB of TiO_2 exit the cell via the TCO substrate, travel through the external circuit and reach the Pt CE. Electron transfer occurs at the Pt CE/electrolyte boundary when the I_3^- ions each receive two electrons from the CE and become I^- ions

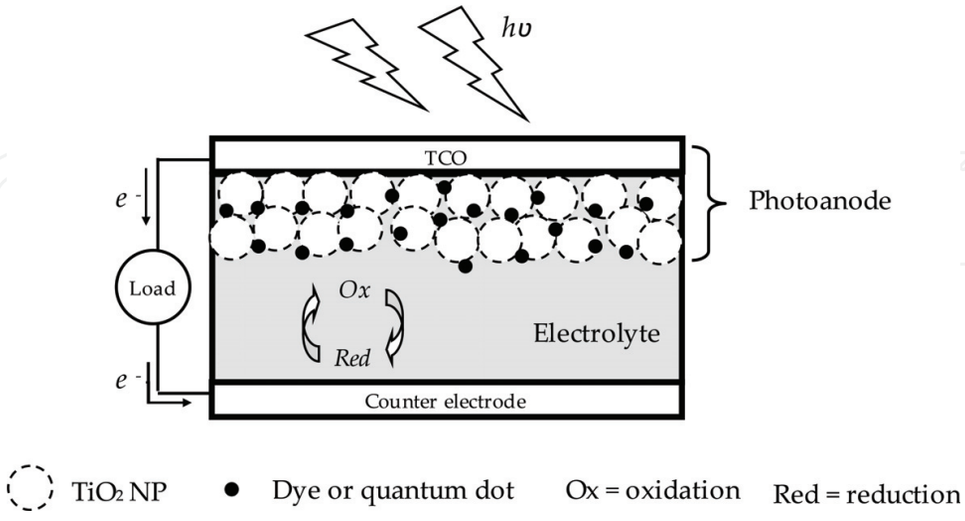

Figure 1. Schematic diagram of DSSC or QDSSC.

(Eq. 4). The I^- ions diffuse back to the photoanode getting oxidized again into I_3^- to complete the circuit. The iodide ions neutralize the ionized dye molecules as shown in Eq. (5):

$$I_3^- + 2e^-{}_{(C.E.)} \rightarrow 3I^- \tag{4}$$

$$2D^+ + 3I^- \rightarrow 2D + I_3^- \tag{5}$$

QDSSC has a similar structure with DSSC except that the sensitizers used are quantum dots (QDs) such as lead sulphide (PbS) [2, 3], cadmium sulphide (CdS) [4, 5], lead selenide (PbSe) [6, 7] and cadmium selenide (CdSe) [8, 9]. Since the I^-/I_3^- couple is corrosive towards QD, it has been replaced with $S^{2-}/S_x{}^{2-}$ couple as the redox mediator in QDSSC. The working principle of QDSSC is the same as DSSC. Electron–hole (*e-h*) pairs are created upon photon absorption by QD (see Eq. 6). Electrons in the CB of the QD are driven into the TiO_2 CB (Eq. 7), and the QD reverts back to its original state when the holes in the QD valence band receive electrons from S^{2-} ions in the electrolyte. An example for a Cd chalcogenide is illustrated in Eq. (8):

$$QD + photons \rightarrow QD\,(e-h) \tag{6}$$

$$QD\,(e+h) + TiO_2 \rightarrow QD(h) + TiO_2(e) \tag{7}$$

$$CdX(h) + S^{2-} \rightarrow CdX + S \tag{8}$$

As in DSSCs, the injected electrons will end up at the CE. S_x^{2-} ion in the electrolyte is then reduced (when it receives 2*e*) to S^{2-} ions. The S^{2-} ions will diffuse back to the photoanode to complete the circuit as shown in Eqs. (9) and (10):

$$S_x{}^{2-} + 2e \rightarrow S_{x-1}{}^{2-} + S^{2-} \tag{9}$$

$$S + S_{x-1}{}^{2-} \rightarrow S_x{}^{2-} \tag{10}$$

The plasmonic NPs can be either deposited on the FTO or ITO surface of the TCO substrate or incorporated in the TiO_2 semiconducting layer of the DSSC and QDSSC (**Figure 2**). However, the studies of plasmonic effect at the CE on the cell performance have also been investigated by some researchers. If the plasmonic NP is embedded in the photoanode, the electrolyte can be either in the solid, gel or liquid state. However, for SPR to occur at the CE and improve

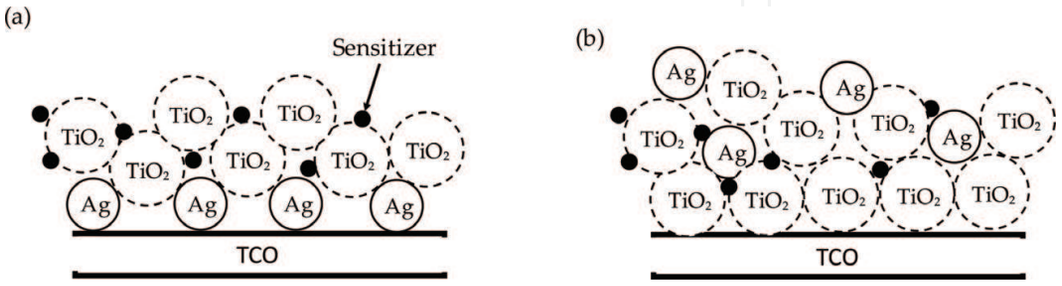

Figure 2. Incorporation of plasmonic NP in photoanode (a) on the surface of TCO and (b) in the semiconductor active layer.

absorption of the sensitizer at the photoanode, the electrolyte must be very thin. Liquid electrolyte is usually used when the NP is deposited at the CE.

4. Performance of DSSC and QDSSC with plasmonic materials incorporated

Table 1 summarizes the performance of DSSC and QDSSC incorporated with plasmonic materials. Gold (Au) and silver (Au) NPs are two most popular plasmonic materials that have been widely used for studying the plasmonic effect on the performance of DSSC and QDSSC.

The most popular method to study the influence of NP on the PV cell characteristics is by introducing the NP in the semiconductor network. An improvement on the efficiency of DSSC from 2.7 to 3.3% was observed by Nahm et al. [10] when 100 nm Au NPs were incorporated into the TiO_2 layer and sensitized with N719 dye. They found that the absorption was stronger in the cell with Au/TiO_2 NP layer than in the cell without Au NPs. This showed that the Au NP plasmonic material helped to increase light absorption, which increased the number of electrons entering the TiO_2 and increased the J_{sc} that led to efficiency improvement. Jun et al. [11] showed that with 5 nm Au NPs, the J_{sc} increased by 65% and efficiency increased from 2.09 to 3.12%. Saravanan et al. [30] studied the plasmonic effect Ag NPs produced from Ag^+ ions treated with *Peltophorum pterocarpum* flower. An efficiency of 3.62% was noted when 2 wt.% of Ag NPs was doped into TiO_2. Efficiency was only 2.83% for the undoped TiO_2. Efficiency increased because of enhancement in light absorption via LSPR, SPP or increased optical pathways. Plasmonic effect on DSSC using phthaloyl chitosan and polyethylene oxide-based gel polymer electrolyte has been studied by Shah et al. [29]. Efficiency enhanced by 13% when Ag NPs were included.

Although efficiency can be enhanced by plasmonic effect, the long-term stability is a major concern, especially when I^-/I_3^- redox mediator was used. This is because the iodide/triiodide couple can corrode the NPs. The presence of NPs in the semiconductor network can also increase recombination process that leads to shorter electron lifetime and lowering of V_{oc} [31]. Due to the high electrical conductivity and the lower work function of the NPs than the CB of TiO_2, the NPs can act as electron recombination centres where electrons that have been driven into TiO_2 re-associated with the holes in the dye molecules or I_3^- ions in the electrolyte. Several efforts have been undertaken to prevent the metal NPs from being corroded. The efforts include utilizing sandwich structure and applying a coating or insulating layer or shell on the surface of the NPs as a protective layer (**Figure 3**).

Sandwich structure (TiO_2/Ag NPs/TiO_2) has been developed by Lin et al. [38] to protect Ag NPs from I^-/I_3^- redox couple. For this sandwich structure, although they have achieved 23% enhancement in Jsc, the Ag NPs are still corroded during the illumination period. Hence, the authors have concluded that applying protective layer on Ag NPs is a necessity. The choice of materials (usually wide bandgap materials) and thickness of the protective layer also influence the performance of DSSC. Brown et al. [15] have incorporated Au NPs coated with silica (SiO_2)

Plasmonic	Semiconductor	Sensitizer	Electrolyte	Performance				Ref.
				J_{sc} (mA/cm^2)	V_{oc} (V)	Efficiency (%)	Efficiency enhancement	
Au NP in active layer	TiO_2	N719 dye	—	5*–6	~0.78	2.7*–3.3	22.2%	[10]
Au NP in active layer	TiO_2	N749 dye	Liquid (I^-/I_3^-)	3.89*–6.42	0.71–0.75*	2.09*–3.12	49.3%	[11]
Au NP in active layer	TiO_2	CdS/ZnS QD	Liquid polysulphide	9.85*–9.48	0.58*–0.61	2.63*–2.96	12.5%	[12]
Au NP in active layer	TiO_2	N719 dye	Liquid (I^-/I_3^-)	18.67*–20.11	0.74*–0.79	9.59–10.8	12.6%	[13]
Au NP in active layer	TiO_2 nanotube	N719 dye	Liquid (I^-/I_3^-)	8.59*–10.25	0.70	3.89*–4.59	18%	[14]
	TiO_2 nanotube/ nanotube photonic crystal	N719 dye	Liquid (I^-/I_3^-)	8.59*–11.71	~0.70	3.89*–5.63	44.7%	
Au@SiO_2 NP in active layer	TiO_2	N719 dye	Liquid (I^-/I_3^-)	2.14*–3.37	~0.74	1.05*–1.95	86%	[15]
		Z907 dye	Hole conductor (spiro-OMeTAD)	3–5*	~0.72	1.2*–2.2	83%	
Au@TiO_2 NP in active layer	TiO_2	N719 dye	Liquid (I^-/I_3^-)	11.55*–14.73	~0.73	6.00*–7.38	23%	[16]
Au@TiO_2 NP in active layer	TiO_2	N719 dye	Liquid (I^-/I_3^-)	18.28	0.73*–0.79	9.29*–9.78	5.3%	[17]
Au@TiO_2 NP in active layer	TiO_2 hollow sphere	N719 dye	Liquid (I^-/I_3^-)	13.6*–22.1	0.72*–0.63	6.25*–8.13	30%	[18]
Au@SiO_2 NP in active layer	TiO_2	N719 dye	Liquid (I^-/I_3^-)	18.28*–20.31	0.73	9.29*–10.21	9.9%	[17]
Au@SiO_2 NP in active layer	TiO_2	N3 dye	Liquid (I^-/I_3^-)	8.25*–10.31	~0.70	3.88*–4.63	19.3%	[19]
		N719 dye	Liquid (I^-/I_3^-)	7.70*–9.80	~0.70	3.52*–4.81	36.6%	
		N749 dye	Liquid (I^-/I_3^-)	5.58*–6.29	0.65	2.41*–2.74	13.7%	
Au nanorod in active layer	TiO_2	N3 dye	—	14.12*–16.19	0.63*–0.65	6.21*–7.29	17.4%	[20]
Au nanorod in active layer	TiO_2	Y123 dye	Liquid (I^-/I_3^-)	12.45*–15.74	0.71*–0.80	5.31*–8.86	66.9%	[21]

Plasmonic	Semiconductor	Sensitizer	Electrolyte	Performance				Ref.
				J_{sc} (mA/cm^2)	V_{oc} (V)	Efficiency (%)	Efficiency enhancement	
Au nanostar in active layer	TiO_2	N719	Liquid (I^-/I_3^-)	15.1*–17.2	0.75* – 0.78	7.00*–8.45	20.7%	[22]
		N749	Liquid (I^-/I_3^-)	8.66*–10.69	0.71* – 0.73	3.53*–5.13	45.3%	
Au@SiO_2 nanorod in active layer	TiO_2	N719	Liquid (I^-/I_3^-)	13.15*–15.88	0.69* – 0.73	5.86*–7.21	23%	[23]
Au@SiO_2@Ag@SiO_2 in active layer	TiO_2	N719	Liquid (I^-/I_3^-)	13.9*–17.58	~ 0.75	7.34*–9.22	25.6%	[24]
Au@Ag@SiO_2 in active layer	TiO_2	N719	Liquid (I^-/I_3^-)	13.89*–16.67	0.68	6.55*–7.72	17.9%	[25]
Au NP on FTO	TiO_2	N719 dye	Liquid (I^-/I_3^-)	11.90*–12.84	~ 0.78	5.84*–6.69	14.6%	[26]
Au NP on FTO	TiO_2	N719 dye	Liquid (I^-/I_3^-)	12.83*–12.34	~ 0.82	6.5*–6.3	Efficiency decreases due to high Schottky barrier	[27]
Au NP on FTO	TiO_2	CdS QD	Liquid polysulphide	5.72*–7.11	0.47* – 0.56	0.86*–1.62	88.4%	[28]
Ag NP in active layer	TiO_2	N3	GPE (I^-/I_3^-)	13.04*–14.74	~0.59	4.61*–5.21	13%	[29]
Ag NP in active layer	TiO_2	Ruthenium N7 dye	Liquid (I^-/I_3^-)	7.52*–8.28	0.63* – 0.71	2.83*–3.62	27.9%	[30]
Ag NP in active layer	TiO_2 nanofiber	N719 dye	Liquid (I^-/I_3^-)	7.57*–9.51	0.8* - 0.78	3.3*–4.13	25%	[31]
Ag NP in active layer	TiO_2	N719 dye	Liquid (I^-/I_3^-)	12.4*–16.20	0.76	7.10*–8.90	25%	[32]
Ag NP in active layer	TiO_2 and ZnO nanorod	CdS and CdSe QDs	Liquid polysulphide	13.27*–15.67	0.70* – 0.74	4.80*–5.92	23.3%	[33]
Ag NP in active layer	ZnO nanorod	CdS QD	Liquid polysulphide	2.18*–3.25	0.59* - 0.63	0.28*–0.60	> 100%	[34]
Ag NP in active layer	TiO_2	N719 dye	Liquid (I^-/I_3^-)	11.97*–15.12	~ 0.73	6.34*–8.05	27%	[35]
Ag NP in active layer	TiO_2 nanorod	N719 dye	—	5.81*–7.11	0.72* – 0.76	1.87*–2.83	51.3%	[36]
Ag NP in electrolyte	TiO_2	N719 dye	Liquid (I^-/I_3^-)	11.97*–12.89	0.73* – 0.76	6.34*–7.11	12%	[35]

http://dx.doi.org/10.5772/intechopen.79580

Plasmonic	Semiconductor	Sensitizer	Electrolyte	Performance				Ref.
				J_{sc} (mA/cm^2)	V_{oc} (V)	Efficiency (%)	Efficiency enhancement	
Polyacrylate modified Ag NP	TiO_2	(Ru(bipy)$_2$(SCN)$_2$ dye	Liquid (I^-/I_3^-)	2.7*–4.40	0.78* - 0.81	1.5*–2.50	66.6%	[37]
Ag NP in active layer—sandwiched structure TiO_2/Ag/TiO_2	TiO_2	N3 dye	Liquid (I^-/I_3^-)	~ 2.7*–6.18	~ 0.83	1.43*–3.01	> 100%	[38]
Ag-ion implantation in active layer	TiO_2 tri-layer	N719 dye	Liquid (I^-/I_3^-)	9.59*–13.04	~ 0.72	4.36*–5.85	34%	[39]
Ag@TiO_2 NP in active layer	TiO_2	N719 dye	Liquid (I^-/I_3^-)	5.12*–6.67	0.66* - 0.69	1.42*–1.83	28.9%	[40]
Ag@TiO_2 NP in active layer	TiO_2	N3 dye		6.07*–8.31	~ 0.8	3.1*–4.4	42%	[41]
Ag@TiO_2 NP in active layer	TiO_2	N719 dye	Liquid (I^-/I_3^-)	7.86*–10.19	0.65* - 0.70	3.95*–5.33	34.9%	[42]
Ag@SiO_2 NP	TiO_2	N719 dye	Liquid (I^-/I_3^-)	10.2*–13.85	0.63* - 0.66	4.30*–6.16	43%	[43]
Ag NP in active layer	Nb-doped TiO_2	N719 dye	Liquid (I^-/I_3^-)	14.1*–16.1	0.73	6.8*–7.6	11.8%	[44]
			Solid (I^-/I_3^-)	11.7*–14.8	0.85	5.4*–6.9	27.8	
Biomass-coated Ag in active layer	TiO_2	N719 dye	Liquid (I^-/I_3^-)	7.48*–11.8	0.76* - 0.79	3.35*–5.12	52.8%	[45]
Ag nanowire in active layer	TiO_2	Beet root	Liquid (I^-/I_3^-)	2.16*–3.60	0.56	0.45*–0.76	68.9%	[46]
		Metal orange	Liquid (I^-/I_3^-)	4.21*–6.77	~ 0.53	1.57*–2.44	55.4%	
Ag nanowire in active layer	TiO_2	N719 dye	Liquid (I^-/I_3^-)	9.69*–11.83	0.71	5.45*–6.26	14.9%	[47]
Ag nanowire@TiO_2	TiO_2	N719 dye	Liquid (I^-/I_3^-)	9.85*–12.01	0.76	4.68*–5.31	13.5%	[48]
Ag nanoplate in active layer	TiO_2	N719 dye	Liquid (I^-/I_3^-)	8.22*–12.47	~ 0.7	2.81*–3.84	36.7%	[49]
Ag@TiO_2 nanocube in active layer	TiO_2	N719 dye	Liquid (I^-/I_3^-)	6.51*–9.54	0.65* – 0.70	2.85*–4.26	49.5%	[50]

Plasmonic	Semiconductor	Sensitizer	Electrolyte	Performance				Ref.
				J_{sc} (mA/cm^2)	V_{oc} (V)	Efficiency (%)	Efficiency enhancement	
Ag NP on FTO	TiO_2	CdSe QD	Liquid polysulphide	5.91*–8.04	0.53* - 0.57	1.05*–1.45	38%	[51]
Ag NP at CE	TiO_2	N719 dye	Liquid (I^-/I_3^-)	15.0*–16.7	~ 0.75	7.60*–8.68	14.2%	[52]
Ag NP at CE	TiO_2	C106 dye	Liquid (I^-/I_3^-)	14.3*–16.5	~ 0.75	6.95*–7.96	14.5%	[53]

N719 = Di-tetrabutylammonium cis-bis(isothiocyanato) bis(2,2′-bipyridyl-4,4′-dicarboxylato) ruthenium(II); N749 = Triisothiocyanato-(2,2′,6′,6″-terpyridyl-4,4′,4″-tricarboxylato) ruthenium(II) tris(tetra-butylammonium); Z907 = Cis-diisothiocyanato-(2,2′-bipyridyl-4,4′-dicarboxylic acid)-(2,2′-bipyridyl-4,4′-dinonyl) ruthenium(II); N3 = Cis-diisothiocyanato-bis(2,2′-bipyridyl-4,4′-dicarboxylic acid) ruthenium(II); Y123 = 3-{6-{4-[bis(2′,4′-dihexyloxybiphenyl-4-yl)amino-]phenyl}-4,4-dihexyl-cyclopenta-[2,1-b,3,4-b′]dithiphene-2-yl}-2-cyanoacrylic acid; C106 = NaRu(4,40-bis(5-(hexylthio)thiophen-2-yl)-2,20-bipyridine)(4-carboxylic acid-40-carboxylate-2,20 -bipyridine)(NCS)2; GPE = Gel polymer electrolyte; J_{sc} = Short-circuit current density; V_{oc} = Open-circuit voltage.
*is the value without metal NPs.

Table 1. Plasmonic DSSC and QDSSC performance.

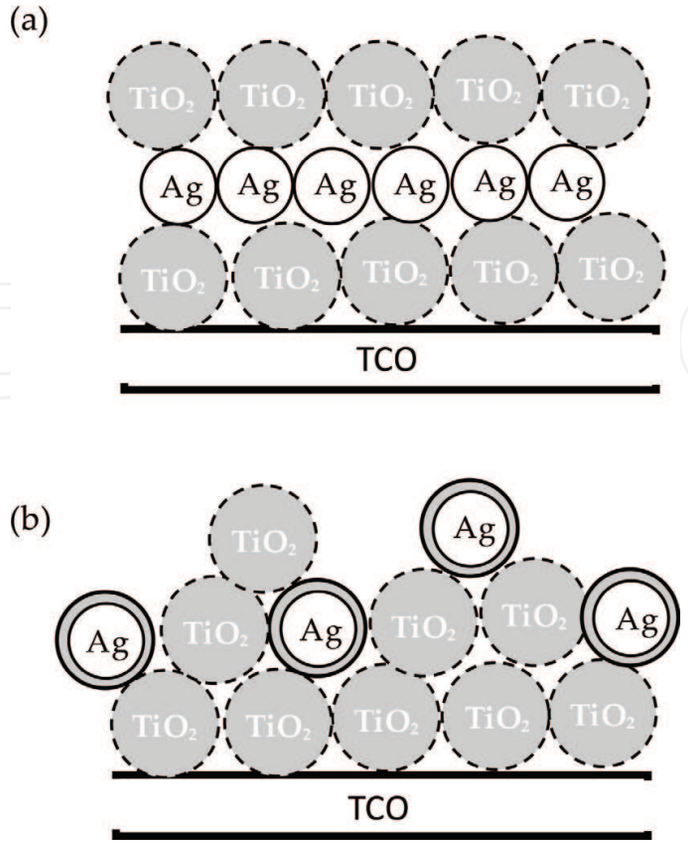

Figure 3. Active layer arrangement to protect metal NPs: (a) TiO_2/Ag sandwich structure and (b) metal core-shell.

layer, metal core-shell nanostructure, into the DSSC. SiO_2 is corrosion resistant towards I^-/I_3^- couple and stable during the sintering process. The authors have employed both I^-/I_3^- redox couple containing liquid electrolyte and spiro-OMeTAD as a medium for charge transportation from cathode to photoanode. Incorporating bare Au NPs in DSSC resulted in lower fill factor, photovoltage and photocurrent due to the metal NPs acting as recombination centres. An increment of about 67% was obtained for photocurrent when the TiO_2 mesoporous layer was incorporated with core-shell Au@SiO_2 NPs and sensitized with Z907 dye. However, due to the insulating nature of SiO_2, the excited dye molecules on SiO_2 have a difficulty in injecting electrons into the SiO_2 coating layer [41]. According to Choi et al. [17], the fact that DSSC with core-shell Au@SiO_2 NPs exhibited higher Jsc is due to surface plasmon effect, while the higher Voc obtained in Au@TiO_2 NPs is attributed to charging effect. In DSSC incorporating core-shell Au@TiO_2, the electrons are more easily injected from dye molecules into TiO_2 compared to SiO_2 and stored in the Au core leading to upward shifting of the TiO_2 Fermi level and increase V_{oc}. The effectiveness of Au NP size on DSSC operation behaviour was studied by Wang et al. [13]. Three different Au NP sizes (5, 45 and 110 nm) were prepared and mixed into a TiO_2 paste before deposition on the FTO or ITO substrate and consequently sensitized with N719 dye. The Au NPs were then protected by additional thin layer of TiO_2. They have observed that smaller-size Au NPs exhibited higher efficiency attributed to the higher V_{oc} which is due to the photocharging effect. Jeong et al. [32] have coated Ag NPs with TiO_2 layer by refluxing

TiO_2/Ag NP electrode in 1.0 M titanium(IV) isopropoxide solution for 25 min. Two layers of TiO_2 NPs with diameter of 18 and 400 nm, respectively, have been deposited by the doctor-blade method. 5 mM $AgNO_3$ in ethanol solution was used to deposit Ag NPs inside the porous TiO_2 by drop-casting technique. From optical studies, the authors inferred that the Ag NPs are elliptical in shape. An improvement of 25% in efficiency was obtained when Ag NPs are included in the photoanode.

The effect of plasmonics in nanostructure oxide semiconductor on QDSSC performance has been studied by Zhao et al. [33]. They have constructed ZnO nanorod electrode doped with Ag and TiO_2 NPs sensitized with CdS and CdSe as shown in **Figure 4**. ZnO nanorods were first grown on FTO glass followed by deposition of Ag and TiO_2 NPs. The complete cell was constructed with polysulphide electrolyte and Cu_2S as cathode. The higher absorption intensity due to LSPR was observed for ZnO/Ag/TiO_2/CdS/CdSe electrode, whereas the absorption intensity for ZnO/TiO_2/CdS/CdSe electrode was lower. An efficiency enhancement of 22% from 4.80 (without Ag NP) to 5.92% (with Ag NP) was obtained. Li et al. [31] have developed TiO_2 nanofiber doped with Ag NPs by electrospinning. The thickness of nanofiber was 15 μm, controlled by the electrospinning time. The authors chose N719 dye to sensitize the TiO_2 nanofiber. The DSSC efficiency increased from 3.3% for undoped DSSC to 4.13% for Ag-doped DSSC. The increased efficiency was attributed to increased J_{sc}. Optical studies revealed that the N719 absorption in Ag-doped semiconductor oxide layer was higher than that of the undoped layer. This is attributed to the strong localized electromagnetic field around the Ag NPs and resulting in higher J_{sc} and efficiency. The authors also found that the electron diffusion coefficient in photoanode increased with Ag-doped DSSC. Eskandari et al. [34] have varied the Ag NP concentration to study the effect on QDSSC performance. The electrolyte used was liquid polysulphide. Different concentrations of Ag NPs (1, 5 and 10%) have been doped into ZnO nanorod array and sensitized with CdS QD as photoanode. Chemical bath deposition (CBD) and successive ion layer absorption and reaction (SILAR) processes were employed for growing ZnO nanorods (NRs) and CdS QDs, respectively. The Ag NPs in their work have been coated with zinc sulphide (ZnS) shell by two-step dipping method. The first step is dipping in 0.05 M

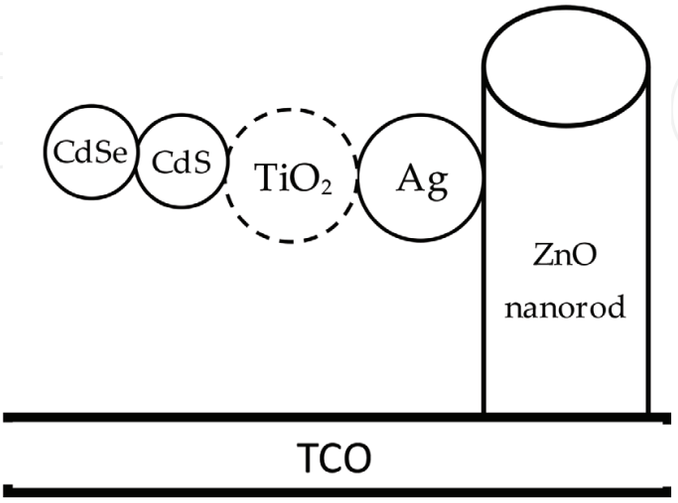

Figure 4. The arrangement of ZnO/Ag/TiO_2/CdS/CdSe electrode [33].

Zn $(CH_3COO)_2.2H_2O$, and the second dipping is in 0.05 M Na_2S solution. Improvements in J_{sc} and V_{oc} were observed when 1 and 5% Ag NPs were embedded in the ZnO NR surface. This is due to LSPR and light scattering. The QDSSC performance dropped for 10% Ag NPs due to the NP corrosion. The authors attributed this to the imperfect coating of the ZnS shell. Guo et al. [42] have prepared several TiO_2 electrodes doped with various quantities (0.05, 0.10, 0.15 and 0.20 wt.%) of Ag@TiO_2 core-shells. The best J_{sc} and V_{oc} combination was obtained when the DSSC was incorporated with 0.15 wt.% Ag@TiO_2 core-shell NPs that subsequently lead to efficiency enhancement of 5.33% from 3.90% for DSSC without Ag@TiO_2 core-shell NPs.

Liu et al. [16] demonstrated the effect of different Au@TiO_2 core-shell NPs on DSSC performance. They found that thicker shell exhibited higher V_{oc}, while higher J_{sc} was produced by thinner shells. Plasmonic DSSCs having Au@TiO_2 with 5 nm shell exhibited efficiency of 7.38% with percentage increment of 23%. Combining Au and Ag NPs have been proposed in order to obtain a broader absorption region. The absorption region between 400 and 550 nm has been noted by Wang et al. [24] for Au coated with Ag and SiO_2. The authors have constructed Au@SiO_2@Ag@SiO_2 NP structure with Au core-coated SiO_2@Ag@SiO_2 shell. The total NP size was about 100 nm. SiO_2 acted as interfacial layer between Au and Ag. It is capable of reducing charge recombination which can be determined by impedance spectroscopy. DSSC fabricated with Au@SiO_2@Ag@SiO_2 electrode exhibited the highest electron lifetime and reported the efficiency as high as 9.22%. Researchers from the same group have also examined how the thickness of Au@Ag@SiO_2 core-shell affects the DSSC operation [25]. The blue shift of absorption peak increased with increasing Ag shell thickness. This has been ascribed to the LSPR effect. The blue shift is due to the dielectric properties of Ag. Optimum efficiency of 7.72% was obtained for DSSC having Ag shell thickness of 15 nm.

The shape of nanoparticles influenced the optical properties. For example, Au with a spherical shape showed the absorption region between 400 and 500 nm, whereas Au nanostars exhibited a strong absorption up to near-infrared (NIR) region (500 nm to 1000 nm) [22]. Approximately 20% enhancement in efficiency from 7.1 (without Au) to 8.4% was obtained when the photoanode contained Au nanostars. Meen et al. [20] have studied the SPR effect of three different shapes of Au NPs (spherical, short and long nanorods) in the photoanode of DSSC. Spherical-shaped Au NPs with average diameter of 45 nm showed absorption peak at 540 nm, whereas the short Au NRs with length:width ratio of 2.5 displayed peaks at 510 and 670 nm. Peaks at 510 and 710 nm were observed for long Au NRs with aspect ratio of 4. The plasmonic bands of NRs are clearly dependent on the aspect ratio. The broader absorption wavelength for long Au nanorods resulted in higher efficiency of 7.29% followed by short Au nanorods and spherical Au with efficiencies of 7.08 and 6.77%, respectively. Without Au NPs, the efficiency of DSSC was only 6.21%. Similar results were obtained by Bai et al. [23] for Au nanorods with aspect ratio of 2.3. Two absorption peaks at 514 and 656 nm were observed. The absorption intensity of Au nanorods coated with SiO_2 is higher compared to that without coating. The efficiency was increased from 5.86% for the DSSC without Au to 7.21% for DSSC with 2.0 wt.% Au. Introduction of Ag@TiO_2 nanocube core-shells into reduced graphene oxide (RGO)-TiO_2 nanotube (NT) has been studied by Chandrasekhar et al. [50]. RGO can increase adsorption surface area and reduce charge recombination rate. Its presence has resulted in a 43% efficiency enhancement from 2.85 to 4.26%. The efficiency was further increased by 21.8% when 0.2 wt.% Ag@TiO_2 core-shell nanocubes were embodied in the photoanode. An increment in J_{sc}

by 22.1% from 9.69 mA/cm^2 and increment of efficiency by 14.9% from 5.45% were achieved when Ag@SiO_2 core-shell nanowire (NW) was applied to the DSSC with N719 dye [47]. Effectiveness of Ag nanowire on the DSSC operation behaviour that utilized natural dye has been investigated by Kazmi et al. [46]. The red shift in absorption spectra of TiO_2-Ag nanowire was observed and attributed to SPR effect. The efficiency of DSSC using Beet root dye is 0.45%, and it was increased to 0.76% in the presence of Ag nanowire.

The interface between TiO_2 and TCO can be modified by depositing metal NP in between TCO and TiO_2. Doosthosseini et al. [51] have deposited Ag NPs on top of FTO glass which acts as interfacial layer followed by a layer of anatase TiO_2 NPs (size = 20 nm) and a layer of rutile TiO_2 NPs (size = 400 nm) sensitized with CdSe QD. The number of SILAR cycles affects the size of the deposited QDs. Since the CB of TiO_2 is higher than the work function of Ag, electrons can be easily collected by the FTO substrate. The Jsc and efficiency of DSSC with Ag NPs as interfacial layer increased from 5.91 mA/cm^2 to 8.04 mA/cm^2 and from 1.05 to 1.45%, respectively. In a similar manner, Zhang et al. [26] have deposited FTO with different sizes of Au NP and by screen printing coating the assembly with TiO_2 NP. The TiO_2 was sensitized with N719 dye. The efficiency increased from 5.84% for without NP deposited FTO to 6.69% for FTO deposited with Au NP. Efficiency enhancement is due to increased Jsc from 11.90 to 12.84 mA/cm^2, and the fill factor increases by 4.9%. According to Ni et al. [54], the performance of DSSC by this arrangement (FTO/ NP/semiconductor) may be explained using the Schottky barrier height model. The Schottky barrier height, φ_b, is dependent on the metal–semiconductor contact. They have formulated the J-V relationship as shown in the following expression:

$$V = \frac{kTm}{q}\ln\left[\frac{(J_{sc}-J)L\cosh(d/L)}{qDn_0\sinh(d/L)}+1\right] - \frac{kT}{q}\ln\left[1+\frac{J}{A*T^2\exp\left(-q\varphi_b/kT\right)}\right] \tag{11}$$

Here, k is 1.38 × 10^{-23} J K^{-1}, T is temperature in kelvins (K), q is 1.602 × 10^{-19} C, m = 2 is ideality factor, D is electron diffusion coefficient and n_0 = 10^{16} cm^{-3} is the dark electron concentration. Further, the electron diffusion length is represented by L, film thickness by d

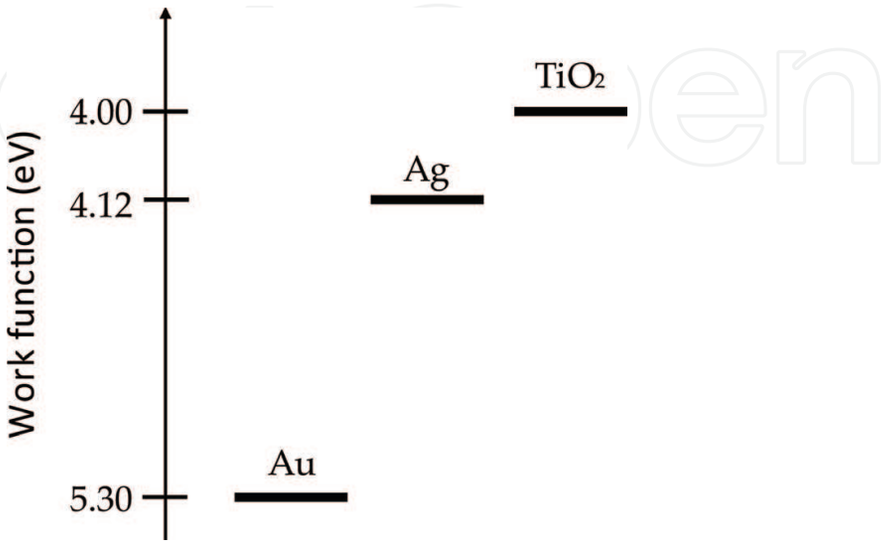

Figure 5. Work function of Au, Ag and TiO_2.

and A^* is the Richardson constant for TiO_2 (6.71×10^6 A m^{-2} K^{-2}). Simulation results show that the fill factor and power output of DSSC are higher when ϕ_b is smaller. The smaller value of ϕ_b implies that the metal–semiconductor is ohmic. Hence, it will be easier for the electrons in CB of TiO_2 to be collected by FTO. Au NP deposited on FTO glass was also studied by Dao and Choi [27]. The J_{sc} and efficiency slightly decreased from 12.82 mA/cm^2 and 6.54% for DSSC without Au NP to 12.34 mA/cm^2 and to 6.27% for FTO deposited with Au NP. However, an increment of J_{sc} and efficiency was observed when the Ag NP was deposited on FTO glass. The efficiency increased to 7.49%. This is due to the higher φ_b in FTO/Au/TiO_2 contact as compared to the FTO/Ag/TiO_2 contact. The work function of Au is 5.3 eV, Ag is 4.12 eV and TiO_2 is 4.0 eV as shown in **Figure 5**.

The effect of plasmonic NP also can be observed when the NP is deposited at CE. The plasmonic effect of Ag NP with three different shapes (prism, sphere and rod) incorporated in Pt CE has been investigated by Ganeshan et al. [52]. They found that the Ag nanorod embedded at Pt CE shows stronger LSPR effect and better scattering property. Hence, 14% enhancement in efficiency was obtained when the Ag/Pt CE is used. About 15% efficiency enhancement was observed by Dong et al. [53] when Au NP was incorporated into CE. This was attributed to the high surface area at CE and the plasmonic effect.

5. Summary

One of the methods to upgrade the optical properties of DSSC and QDSSC components is by incorporating DSSC and QDSSC NPs which lead to better efficiency. These materials can be incorporated in the photoanode and counter electrode of the cells. Both methods improved light absorption efficiency. Different types, shapes, concentrations and sizes of NPs contributed to the plasmonic effect.

Acknowledgements

The authors would like to thank the University of Malaya and the Malaysian Ministry of Higher Education (MOHE) for the financial support (FG029-17AFR and FP053-2016).

Author details

Abdul Kariem Bin Mohd Arof* and Mohd Hamdi Bin Ali Buraidah

*Address all correspondence to: akarof@um.edu.my

Centre for Ionics University of Malaya, Department of Physics, Faculty of Science, University of Malaya, Kuala Lumpur, Malaysia

References

[1] Gangadharan DT, Xu Z, Liu Y, Izquierdo R, Ma D. Recent advancement in plasmon-enhanced promising third-generation solar cells. Nano. 2017;**6**:153-175

[2] Lee HJ, Chen P, Moon S-J, Sauvage F, Sivula K, Bessho T, Gamelin DR, Comte P, Zakeeruddin SM, Il SS, Grätzel M, Nazeeruddin MK. Regenerative PbS and CdS quantum dot sensitized solar cells with a cobalt complex as hole mediator. Langmuir. 2009;**25**:7602-7608

[3] Heo JH, Jang MH, Lee MH, Shin DH, Kim DH, Moon SH, Kim SW, Park BJ, Im SH. High-performance solid-state PbS quantum dot-sensitized solar cells prepared by introduction of hybrid Perovskite interlayer. ACS Applied Materials & Interfaces. 2017;**9**:41104-41110

[4] Lee Y-S, Gopi CVVM, Reddy AE, Nagaraju C, Kim H-J. High performance of TiO_2/CdS quantum dot sensitized solar cells with a Cu–ZnS passivation layer. New Journal of Chemistry. 2017;**41**:1914-1917

[5] Jun HK, Careem MA, Arof AK. Performances of some low-cost counter electrode materials in CdS and CdSe quantum dot-sensitized solar cells. Nanoscale Research Letters. 2014;**9**:69

[6] Zhang J, Gao J, Church CP, Miller EM, Luther JM, Klimov VI, Beard MC. PbSe quantum dot solar cells with more than 6% efficiency fabricated in ambient atmosphere. Nano Letters. 2014;**14**:6010-6015

[7] Kim S, Marshall AR, Kroupa DM, Miller EM, Luther JM, Jeong S, Beard MC. Air-stable and efficient PbSe quantum-dot solar cells based upon ZnSe to PbSe Cation-exchanged quantum dots. ACS Nano. 2015;**9**:8157-8164

[8] Huang F, Zhang L, Zhang Q, Hou J, Wang H, Wang H, Peng S, Liu J, Cao G. High efficiency CdS/CdSe quantum dot sensitized solar cells with two ZnSe layers. ACS Applied Materials & Interfaces. 2016;**8**:34482-34489

[9] Pandi DV, Muthukumarasamy N, Agilan S, Velauthapillai D. CdSe quantum dots sensitized ZnO nanorods for solar cell application. Materials Letters. 2018;**223**:227-230

[10] Nahm C, Choi H, Kim J, Jung D-R, Kim C, Moon J, Lee B, Park B. The effects of 100 nm-diameter Au nanoparticles on dye-sensitized solar cells. Applied Physics Letters. 2011;**99**:253107

[11] Jun HK, Careem MA, Arof AK. Plasmonic effects of quantum size gold nanoparticles on dye-sensitized solar cell. Materials Today: Proceedings. 2016;**3S**:S73-S79

[12] Zarazúa I, Esparza D, López-Luke T, Ceja-Fdez A, Reyes-Gomez J, Mora-Seró I, de la Rosa E. Effect of the electrophoretic deposition of Au NPs in the performance CdS QDs sensitized solar cells. Electrochimica Acta. 2016;**188**:710-717

[13] Wang Q, Butburee T, Wu X, Chen H, Liu G, Wang L. Enhanced performance of dye-sensitized solar cells by doping Au nanoparticles into Photoanodes: A size effect study. Journal of Materials Chemistry A. 2013;**1**:13524-13531

[14] Guo M, Chen J, Zhang J, Su H, Liu L, Fu N, Xie K. Coupling plasmonic nanoparticles with TiO_2 nanotube photonic crystals for enhanced dye-sensitized solar cells performance. Electrochimica Acta. 2018;**263**:373-381

[15] Brown MD, Suteewong T, Kumar RSS, D'Innocenzo V, Petrozza A, Lee MM, Wiesner U, Snaith HJ. Plasmonic dye-sensitized solar cells using Core-Shell metal-insulator nanoparticles. Nano Letters. 2011;**11**:438-445

[16] Liu W-L, Lin F-C, Yang Y-C, Huang C-H, Gwo S, Huang MH, Huang J-S. The influence of shell thickness of Au@TiO_2 core–shell nanoparticles on the plasmonic enhancement effect in dye-sensitized solar cells. Nanoscale. 2013;**5**:7953-7962

[17] Choi H, Chen WT, Kamat PV. Know thy nano neighbor. Plasmonic versus Electron charging effects of metal nanoparticles in dye-sensitized solar cells. ACS Nano. 2012;**6**:4418-4427

[18] Du J, Qi J, Wang D, Tang Z. Facile synthesis of Au@TiO_2 core–shell hollow spheres for dye-sensitized solar cells with remarkably improved efficiency. Energy & Environmental Science. 2012;**5**:6914-6918

[19] Li H, Hong W, Cai F, Tang Q, Yan Y, Hu X, Zhao B, Zhang D, Xu Z. Au@SiO_2 nanoparticles coupling co-sensitizers for synergic efficiency enhancement of dye sensitized solar cells. Journal of Materials Chemistry. 2012;**22**:24734-24743

[20] Meen T-H, Tsai J-K, Chao S-M, Lin Y-C, Wu T-C, Chang T-Y, Ji L-W, Water W, Chen W-R, Tang I-T, Huang C-J. Surface plasma resonant effect of gold nanoparticles on the photoelectrodes of dye-sensitized solar cells. Nanoscale Research Letters. 2013;**8**:450

[21] Chandrasekhar PS, Parashar PK, Swami SK, Dutta V, Komarala VK. Enhancement of Y123 dye-sensitized solar cells performance using plasmonic gold nanorods. Physical Chemistry Chemical Physics. 2018;**20**:9651-9658

[22] Elbohy H, Kim MR, Dubey A, Reza KM, Ma D, Zai J, Qian X, Qiao Q. Incorporation of plasmonic Au nanostars into photoanodes for high efficiency dye sensitized solar cells. Journal of Materials Chemistry. 2016;**A4**:545-551

[23] Bai L, Li M, Guo K, Luoshan M, Mehnane HF, Pei L, Pan M, Liao L, Zhao X. Plasmonic enhancement of the performance of dye-sensitized solar cell by core-shell AuNRs@SiO_2 in composite photoanode. Journal of Power Sources. 2014;**272**:1100-1105

[24] Wang Y, Zhai J, Song Y, Lin J, Yin P, Guo L. Interfacial effect of novel Core–triple Shell structured Au@SiO_2@Ag@SiO_2 with ultrathin SiO_2 passivation layer between the metal interfaces on efficient dye-sensitized solar cells. Advanced Materials Interfaces. 2015;**2**: 1500383

[25] Wang Y, Zhai J, Song Y, He L. Ag Shell thickness effect of Au@Ag@SiO_2 Core-Shell nanoparticles on optoelectronic performance for dye sensitized solar cells. Chemical Communications. 2016;**52**:2390-2393

[26] Zhang D, Wang M, Brolo AG, Shen J, Li X, Huang S. Enhanced performance of dye-sensitized solar cells using gold nanoparticles modified fluorine tin oxide electrodes. Journal of Physics D: Applied Physics. 2013;**46**:024005

[27] Dao V-D, Choi H-S. Highly-efficient Plasmon-enhanced dye-sensitized solar cells created by means of dry plasma reduction. Nanomaterials. 2016;**6**:70. DOI: 10.3390/nano6040070

[28] Zhu G, Su F, Lv T, Pan L, Sun Z. Au nanoparticles as interfacial layer for CdS quantum dot-sensitized solar cells. Nanoscale Research Letters. 2010;**5**:1749-1754

[29] Shah S, Noor IM, Pitawala J, Albinson I, Bandara TMWJ, Mellander B-E, Arof AK. Plasmonic effects of quantum size metal nanoparticles on dye-sensitized solar cell. Optical Materials Express. 2017;**7**:2069-2083

[30] Saravanan S, Kato R, Balamurugan M, Kaushik S, Soga T. Efficiency improvement in dye sensitized solar cells by the plasmonic effect of green synthesized silver nanoparticles. Journal of Science: Advanced Materials and Devices. 2017;**2**:418-424

[31] Li J, Chen X, Ai N, Hao J, Chen Q, Strauf S, Shi Y. Silver nanoparticle doped TiO_2 nanofiber dye sensitized solar cells. Chemical Physics Letters. 2011;**514**:141-145

[32] Jeong NC, Prasittichai C, Hupp JT. Photocurrent enhancement by surface Plasmon resonance of silver nanoparticles in highly porous dye-sensitized solar cells. Langmuir. 2011; **27**:14609-14614

[33] Zhao H, Huang F, Hou J, Liu Z, Wu Q, H-b C, Jing Q, Peng S, Cao G. Efficiency enhancement of quantum dot sensitized TiO_2/ZnO nanorod arrays solar cells by plasmonic Ag nanoparticles. ACS Applied Materials & Interfaces. 2016;**8**:26675-26682

[34] Eskandari M, Ahmadi V, Yousefi rad M, Kohnehpoushi S. Plasmon enhanced CdS-quantum dot sensitized solar cell using ZnO nanorods array deposited with Ag nanoparticles as photoanode. Physica E: Low-dimensional Systems and Nanostructures. 2015;**68**:202-209

[35] Adhyaksa GWP, Baek S-W, Lee GI, Lee DK, Lee JY, Kang JK. Coupled near- and far-field scattering in silver nanoparticles for high-efficiency, stable, and thin Plasmonic dye-sensitized solar cells. ChemSusChem. 2014;**7**:2461-2468

[36] Hu H, Shen J, Cao X, Wang H, Lv H, Zhang Y, Zhang W, Zhao J, Cui C. Photo-assisted deposition of Ag nanoparticles on branched TiO_2 nanorod arrays for dye-sensitized solar cells with enhanced efficiency. Journal of Alloys and Compounds. 2017;**694**:653-661

[37] Ihara M, Kanno M, Inoue S. Photoabsorption-enhanced dye-sensitized solar cell by using localized surface plasmon of silver nanoparticles modified with polymer. Physica E: Low-dimensional Systems and Nanostructures. 2010;**42**:2867-2871

[38] Lin S-J, Lee K-C, Wu J-L, Wu J-Y. Enhanced performance of dye-sensitized solar cells via plasmonic sandwiched structure. Applied Physics Letters. 2011;**99**:043306

[39] Luo J, Zhou J, Guo H, Yang W, Liao B, Shi W, Chen Y. Effects of Ag-ion implantation on the performance of DSSCs with a tri-layer TiO_2 films. RSC Advances. 2014;**4**:56318-56322

[40] Zhang X, Liu J, Li S, Tan X, Yu M, Du J. Bioinspired synthesis of Ag@TiO_2 plasmonic nanocomposites to enhance the light harvesting of dye sensitized solar cells. RSC Advances. 2013;**3**:18587-18595

[41] Qi J, Dang X, Hammond PT, Belcher AM. Highly efficient Plasmon-enhanced dye-sensitized solar cells through metal@oxide CoreShell nanostructure. ACS Nano. 2011;**5**: 7108-7116

[42] Guo K, Li M, Fang X, Liu X, Sebo B, Zhu Y, Hu Z, Zhao X. Preparation and enhanced properties of dye-sensitized solar cells by surface plasmon resonance of Ag nanoparticles in nanocomposite photoanode. Journal of Power Sources. 2013;**230**:155e160

[43] Hossain MA, Park J, Yoo D, Baek Y, Kim Y, Kim SH, Lee D. Surface plasmonic effects on dye-sensitized solar cells by SiO_2-encapsulated Ag nanoparticles. Current Applied Physics. 2016;**16**:397-403

[44] Park JT, Chi WS, Jeon H, Kim JH. Improved electron transfer and plasmonic effect in dye-sensitized solar cells with bi-functional Nb doped TiO_2/Ag ternary nanostructures. Nanoscale. 2014;**6**:2718-2729

[45] Tian Z, Wang L, Jia L, Li Q, Song Q, Su S, Yang H. Photoanode for enhanced photocurrent in dye sensitized solar cells. RSC Advances. 2013;**3**:6369-6376

[46] Kazmi SA, Hameed S, Azam A. Synthesis and characterization of Ag nanowires: Improved performance in dye sensitized solar cells. Perspectives in Science. 2016;**8**:577-579

[47] Guo K, Li M, Fang X, Liu X, Zhu Y, Hu Z, Zhao X. Enhancement of properties of dye-sensitized solar cells by surface plasmon resonance of Ag nanowire core–shell structure in TiO_2 films. Journal of Materials Chemistry A. 2013;**1**:7229-7234

[48] Huang P-C, Chen T-Y, Wang Y-L, Wua C-Y, Lin T-L. Improving interfacial electron transfer and light harvesting in dye-sensitized solar cells by using Ag nanowire/TiO_2 nanoparticle composite films. RSC Advances. 2015;**5**:70172-70177

[49] Hwang H-J, Joo S-J, Patil SA, Kim H-S. Efficiency enhancement in dye-sensitized solar cells using the shape/size-dependent plasmonic nanocomposite photoanodes incorporating silver nanoplates. Nanoscale. 2017;**9**:7960-7969

[50] Chandrasekhar PS, Chander N, Anjaneyulu O, Komarala VK. Plasmonic effect of Ag@TiO_2 core–shell nanocubes on dye-sensitized solar cell performance based on reduced graphene oxide–TiO_2 nanotube composite. Thin Solid Films. 2015;**594**:45-55

[51] Doosthosseini F, Behjat A, Hashemizadeh S, Torabi N. Application of silver nanoparticles as an interfacial layer in cadmium sulfide quantum dot sensitized solar cells. Journal of Nanophotonics. 2015;**9**:093092

[52] Ganeshan D, Xie F, Sun Q, Li Y, Wei M. Plasmonic effects of silver nanoparticles embedded in the counter electrode on enhanced performance of dye-sensitized solar cells. Langmuir. 2018;**34**:5367-5373

[53] Dong H, Wu Z, Gao Y, El-Shafei A, Jiao B, Dai Y, Hou X. A nanostructure based counter electrode for dye-sensitized solar cells by assembly of silver nanoparticles. Organic Electronics. 2014;**15**:1641-1649

[54] Ni M, Leung MKH, Leung DYC, Sumathy K. Theoretical modeling of TiO_2/TCO interfacial effect on dye-sensitized solar cell performance. Solar Energy Materials & Solar Cells. 2006;**90**:2000-2009

IntechOpen